Abdominal Radiology

Published online: 12 October 2018

Abdom Radiol (2019) 44:950–957
https://doi.org/10.1007/s00261-018-1791-x

PET/CT in brachytherapy early response evaluation of pancreatic ductal adenocarcinoma xenografts: comparison with apparent diffusion coefficient from diffusion-weighted MR imaging

Yu Liu,[1] Min Liu,[2] Xiaona Liu,[3] and Yan Zhou[3]

[1]Department of Radiology, Ninth People's Hospital, Shanghai Jiao Tong University School of Medicine, Shanghai, China
[2]Department of CT, The People's Hospital of Xiang Yun, Bai Autonomous Region, Dali, Yunnan, China
[3]Yantai Affiliated Hospital of Binzhou Medical University, Shandong, China

Abstract

Objective: To evaluate the feasibility of using PET/CT and diffusion-weighted magnetic resonance imaging (DW-MRI) to monitor the early response of pancreatic ductal adenocarcinoma (PDAC) xenografts to brachytherapy, and to determine whether maximum standardized uptake value (SUVmax) correlate with apparent diffusion coefficient (ADC).

Materials and Methods: SW1990 human PDAC were subcutaneously implanted in 20 nude mice. They were randomly divided into 125-Iodine (^{125}I) seeds and blank seeds group. PET/CT and DW-MRI were performed at pretreatment and 5 days after therapy. SUVmax and ADC values were calculated, respectively. The correlation between SUVmax and ADC values was analyzed by the Pearson correlation test.

Results: The SUVmax were significantly decreased between pretreatment and 5 days after ^{125}I seeds treatment ($p < 0.001$) and between two groups ($p < 0.001$). And the ADC values were significantly increased between pretreatment and 5 days after ^{125}I seeds treatment ($p < 0.001$) and between two groups ($p < 0.001$). While in the bank seeds group, there were no significantly difference between pretreatment and after treatment in SUVmax and ADC values ($p = 0.057$; $p = 0.397$). SUVmax and ADC correlated significantly and negatively before treatment in both groups ($r = -0.964$, $R^2 = 0.929$, $p < 0.001$; $r = -0.917$, $R^2 = 0.841$, $p < 0.001$) and after treatment in the blank seeds group ($r = -0.944$, $R^2 = 0.891$, $p < 0.001$). But after ^{125}I seeds treatment there was no significant correlation between SUVmax and ADC ($r = -0.388$, $R^2 = 0.151$, $p = 0.268$).

Conclusion: The PET/CT and DW-MRI are capable of monitoring the early response of PDAC xenografts to brachytherapy. The significantly inverse correlation between pretreatment SUVmax and ADC suggests that PET/CT and DW-MRI might play complementary roles for therapy assessment.

Key words: Iodine-125 seeds—Brachytherapy—Pancreatic ductal adenocarcinoma—Xenografts—^{18}F-FDG PET/CT—Diffusion-weighted MRI

The pancreatic ductal adenocarcinoma (PDAC) is a highly malignant digestive tumor with poor prognosis. The early surgical resection is the only possible cure for PDAC. But because its clinical symptoms are hidden and not specific, PDAC is usually advanced and not resectable at the first diagnosis. For the advanced PDAC, a variety of therapies are used, such as radiotherapy, chemotherapy, and targeted therapies. While each therapy has its limitation, such as radiotherapy may cause damage to normal organs adjacent the tumor, chemotherapy may have systemic side effects, and targeted therapy is expensive, and its curative effect also varies from person to person. In recent years, it is reported that the Iodine-125 (^{125}I) seeds brachytherapy has been effective in the treatment of advanced PDAC [1]. ^{125}I seeds is a radioactive particle source. It can consistently emit low-dose X-rays and gamma in r-rays with the short effective penetration distance and long half-life time. So it can focus on the lesion avoiding radiation

Yu Liu and Min Liu have contributed equally to this work.

Correspondence to: Yu Liu; *email:* yliu9y@126.com

damage to the surrounding normal organs and play a consistent role for a long time.

Molecular imaging makes noninvasive evaluation of response to therapy possible. ^{18}F-fluorodeoxyglucose positron emission tomography/computed tomography (^{18}F-FDG PET/CT) reflects tumor metabolic activity which contributes to diseases diagnosis and differential diagnosis between benign and malignant tumors [2]. And it is a sensitive assessment modality for therapy response to radiation, chemotherapy, and targeted therapies [3–5]. The maximum standardized uptake value (SUVmax) can semiquantitatively assess glucose metabolism. The SUVmax changes have been reported to be useful in the diagnosis, staging, efficacy evaluation, and prognosis in pancreatic lesions [2]. And functional MRI is another important modality for therapy response. Diffusion-weighted magnetic resonance imaging (DW-MRI) measures the random motion of free water molecules potentially reflecting tissue cellularity [6]. The apparent diffusion coefficient (ADC) calculated by DW-MRI is used to quantify local water diffusion. The ADC values usually decrease in malignant tumors because of their inverse relationship with tissue cellularity. The ADC values changes also have been reported to be useful in monitoring therapeutic response of PDAC. And changes in FDG uptake and ADC values have been reported to precede tumor size in early assessment of treatment effects [7].

To our knowledge, there is no reported study comparing the brachytherapy efficacy assessment by ^{18}F-FDG PET/CT and DW-MRI in PDAC xenografts. Thus in this study, we investigated whether early response assessment of brachytherapy using these imaging biomarkers is feasible. And we also investigated the correlation between SUVmax and ADC.

Materials and methods

PDAC xenografts model

Animal experiments were reviewed and approved by the Institutional Animal Care and Use Committee of the local hospital.

Twenty 4-week-old BALB/c male nude mice bought from the University School of Medicine Experimental Animal Center were implanted subcutaneously SW 1990 cell suspension (1×10^7 cells/mL, 0.4 mL) into the flank near the lower limb. We used a caliper to measure the tumor size. When the tumor diameter reached 8–10 mm, they underwent ^{18}F-FDG PET/CT and DW-MRI pretreatment and 5 days after seeds implantation. The mice were randomly divided into two groups. One ^{125}I seed (0.5 mCi) purchased from GMS Pharmaceutical Co. Ltd was implanted into the center of tumor by the 18-gauge needle as the treatment group ($n = 10$), and one blank seed (0 mCi) as control group ($n = 10$).

^{18}F-FDG PET/CT protocol

PET/CT examinations were performed on small animal Micro-PET/CT scanners (Inveon, Siemens, Healthcare, Germany). Imaging studies were conducted before therapy (baseline), and 5 days after therapy. Animals were routinely fasted for 6 h prior to ^{18}F-FDG injection. During imaging, all animals were anesthetized using isoflurane gas (1%–2%) and the temperature of animal bed was maintained to 37°C. 7.4 MBq ^{18}F-FDG was administered intravenously. After 60 min injection, the static PET imaging was acquired for 20 min. CT images prior to the PET scans were performed with the following parameters: voltage of X-ray tube, 80 kVp; the tube current, 0.5 mA; axial field of view, 80 mm; acquisition time, 10 min per animal [8]. Images were analyzed using the software Inveon Research Workplace 3.0 (Siemens Medical Solutions). A manually defined three-dimensional range of interest covered the entire tumor. On PET images, the SUV was calculated as followed: SUV = tissue activity concentration (MBq/mL) * animal body weight (g)/activity concentration (MBq/mL) [9]. The SUVmax was measured as the maximum value of SUV in each voxel within the three-dimensional volumes of interest of tumors.

MRI protocol

MR examinations were performed on a 1.5T MR imaging system using a 3-inch surface coil (HD SIGNA EXCITE, GE, U.S.A). All animals were anesthetized using isoflurane gas (1%–2%) during imaging. The mouse was covered with a thin quilt to prevent hypothermia. Imaging acquisition was conducted before therapy (baseline), and 5 days after therapy. DW-MRI was performed using single shot echo-planar sequences with fat suppression with the following acquisition parameters: (b values = 0 and 500 s/mm^2; repetition time msec (TR)/echo time msec (TE) = 2200/75.8; diffusion separation time = 16 ms; diffusion gradient duration = 6 ms; matrix = 64 × 64; field of view (FOV) = 80 × 40 mm; slice thickness = 1.8 mm, and slice gap = 0.2 mm; scan time = 1 min and 28 s) [10]. ADC values were calculated automatically by the MR Functool 2 analysis software in offline workstation (ADW 4.4, GE Healthcare, USA). Regions of interests (ROIs) were manually defined enveloping the peripheral zone of tumors without seeds in the ADC map.

Histologic analysis

After ^{18}F-FDG PET/CT and DW-MRI scans, all mice were euthanized. The tumor specimens were fixed in 4% formalin for 24–48 h, dehydrated, and embedded in paraffin. And thin sections (5 μm) were collected and used for histological analysis with hematoxylin and eosin

(H&E) staining [5]. And the H&E stained slides were reviewed by a senior pathologist. The amount of necrosis was calculated as the proportion (percentage of total tumor area) of necrosis.

Statistical analysis

All statistical analysis was processed using SPSS 13.0 software (SPSS Inc., Chicago, IL). All qualitative data were presented as mean ± SD. A paired Student's *t* test was used to compare the SUVmax and ADC values of tumor in the same group at each time point. And an independent Student's *t* test was used to compare the SUVmax and ADC values of tumor between two groups at each time point. Pearson correlation was used to analyze the relationships between the SUVmax and ADC values at each time point. Differences were considered significant when the two-sided *p* values were less than 0.05.

Results

SUVmax on ^{18}F-FDG PET/CT

All nude mice bearing tumor completed the ^{18}F-FDG PET/CT scan with minimal motion artifact. On ^{18}F-FDG PET/CT, the tumor parenchyma presented high FDG uptake, tumor necrosis region showed no obvious FDG uptake, and seeds showed no FDG uptake with a small amount of CT hardening artifact (Fig. 1). Table 1 shows the comparison of SUVmax between the ^{125}I seeds group and the blank seeds group at baseline and 5 days after therapy. The SUVmax showed no significant difference between two groups at baseline ($p = 0.295$). After ^{125}I seeds implantation, the SUVmax were significantly decreased compared with baseline ($p < 0.001$) and with the blank seeds group ($p < 0.001$). While in the blank seeds group, the SUVmax changed from 1.253 ± 0.3096 to 1.430 ± 0.4296, but there were no significant differences between baseline and 5 days after implantation ($p = 0.057$).

ADC values on DW-MRI

All nude mice bearing tumor completed the DW-MRI with minimal motion artifact. PDAC xenografts showed high signal intensity on DW-MRI and low signal intensity on ADC maps with the no signal seeds (Fig. 2). Table 1 also shows the comparison of ADC values between the ^{125}I seeds group and the blank seeds group at baseline and 5 days after therapy. The ADC values showed no significant difference between two groups at baseline ($p = 0.803$). After ^{125}I seeds implantation, the ADC values were significantly increased compared with baseline ($p < 0.001$) and with the blank seeds group ($p < 0.001$). While in the blank seeds group, the ADC values showed no significant differences between baseline and 5 days after implantation ($p = 0.397$).

Relationship between SUVmax and ADC values

The SUVmax were significantly and negatively correlated to ADC values before treatment in both groups ($r = -0.964$, $R^2 = 0.929$, $p < 0.001$; $r = -0.917$, $R^2 = 0.841$, $p < 0.001$). And the results showed significantly negative correlation between SUVmax and ADC values after treatment in the blank seeds group ($r = -0.944$, $R^2 = 0.891$, $p < 0.001$). However, after ^{125}I seeds treatment there was no significant correlation between SUVmax and ADC values($r = -0.388$, $R^2 = 0.151$, $p = 0.268$).

Histological results

H&E staining showed that in the ^{125}I seeds group there was significant necrosis around seeds with no cell structure and the residual tumor cells arranged loosely and appeared karyopyknosis (Fig. 3a). But in the blank seeds group the tumor tissue showed no or a small amount of necrotic area, the tumor cells arranged closely, cells nuclear deeply dyed, and appeared more mitotic activity (Fig. 3b). And the animals who received ^{125}I seeds brachytherapy, compared with the control, had higher percentage of necrosis (mean: $82.0 \pm 6.75\%$ vs. $6.1 \pm 5.04\%$, $p < 0.001$).

Discussion

Recently, brachytherapy with ^{125}I seeds is an important therapeutic measures for patients with advanced and unresectable malignant tumors, tumors insensitive to chemotherapy, or metastatic tumors [1, 11]. Brachytherapy with ^{125}I seeds for prostate cancer has a favorable medium-term effect and retains its physiological function [11]. In recent years, brachytherapy with ^{125}I seeds has been used in the treatment of advanced PDAC, and has achieved a certain clinical efficacy [1]. The biological behavior of ^{125}I seeds is as follows: they can consistently emit low-energy X-rays and r-rays, low penetration for 17 mm soft tissues, and long half-time for 59.6 days. Therefore, their radiation doses can focus on the tumors killing the tumor cells without injury to adjacent normal organs. And persistent low-dose exposure can significantly increased the biological effect on tumor tissue, and lead to complete destruction of DNA, cell apoptosis, and necrosis [12]. Our histological results conformed ^{125}I seeds could lead to significant necrosis with no cell structure. Clinically, the implantation of ^{125}I seeds can be guided by CT and B-ultrasound with a minimally invasively percutaneous approach or directly implant during operation. To evaluate the efficacy of

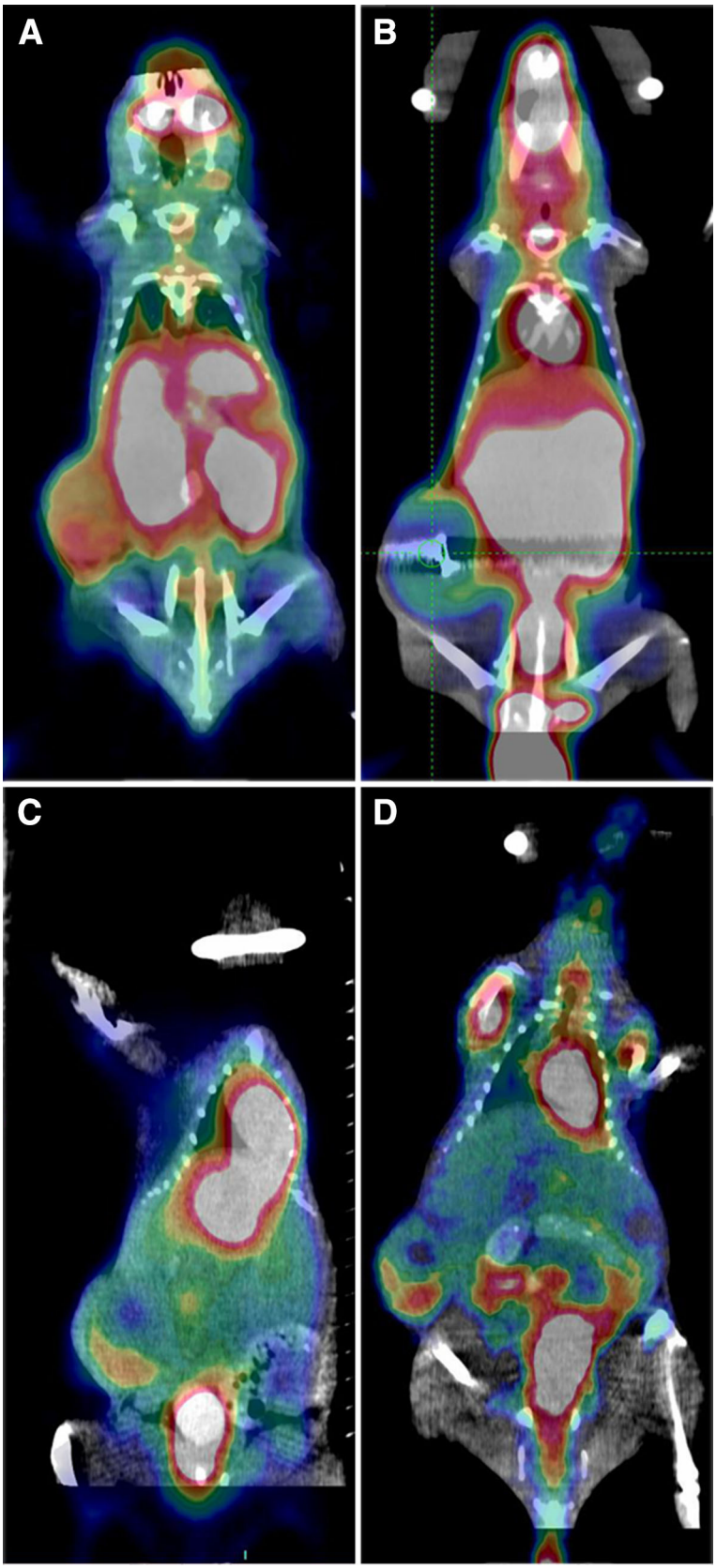
A
B
C
D

◀**Fig. 1.** The FDG uptake on the ^{18}F-FDG PET/CT. **A** Tumor parenchyma presented high FDG uptake before treatment in the ^{125}I seeds group. **B** After the ^{125}I seeds brachytherapy, tumor necrosis region showed no obvious FDG uptake, and seeds showed no FDG uptake with a small amount of CT hardening artifact. **C** Tumor presented high FDG uptake with spot necrosis with no FDG uptake in the control group. **D** The FDG uptake slightly increased after 5 days in the control group.

Table 1. The mean SUVmax and ADC values in ^{125}I seeds group and control group in each time point

	^{125}I seeds group Mean ± SD	Control group Mean ± SD	*p* value
SUVmax			
Day 0	1.447 ± 0.4776	1.253 ± 0.3096	0.295
Day 5	0.334 ± 0.1697	1.430 ± 0.4296	< 0.001
ADC			
Day 0	0.000813 ± 0.0001705	0.000793 ± 0.0001818	0.803
Day 5	0.001139 ± 0.0000953	0.000837 ± 0.0001443	< 0.001

Data are the mean ± SD
Day 0, before treatment; Day 5, after 5 days of initiating treatment; ADC, apparent diffusion coefficient, mm^2/s; SUVmax, maximum standardized uptake value

brachytherapy with ^{125}I seeds for PDAC, the previous morphologic evaluation of tumor size has not been sufficient to evaluate the response. We designed an animal trial of PDAC, and attempted to evaluate the efficacy of ^{125}I seeds brachytherapy for PDAC from molecule levels by noninvasive and functional imaging modalities.

^{18}F-FDG PET/CT is a functional imaging mentality that provides unique molecular and metabolic information based on glucose uptake. Clinically, ^{18}F-FDG PET/CT is increasingly used in patients with PDAC for preoperative diagnosis, staging, lymph node and distant metastasis, as well as early therapy response evaluation [2]. In animal studies, Micro-PET/CT has also been used for early PDAC detection and efficacy evaluation [13]. Some studies have shown that SUVmax is a valuable parameter for monitoring and evaluating the efficacy of PDAC [2]. We use Micro-PET/CT to monitor the ^{125}I seeds brachytherapy for PDAC xenografts. In our study, all PDAC xenografts showed high FDG uptake on ^{18}F-FDG PET/CT images. And after the ^{125}I seeds brachytherapy for PDAC xenografts, the ^{18}F-FDG uptake decreased significantly. While in the control group the FDG uptake showed a tendency of increase even though without statistical differences. These results suggested that ^{125}I seeds brachytherapy had anti-tumor effect and was able to effectively inhibit tumor cell proliferation. Shah et al. [9] used ^{18}F-FDG PET/CT to evaluate the therapeutic response anti-EMMPRIN in PDAC xenografts, and got the similar results that the ^{18}F-FDG uptake decreased.

Moreover, we used ADC values provided by DW-MRI to evaluate the brachytherapy response. ADC is reported as a valuable biomarker to reflect tumor cell density. The high tumor cell density can increase extracellular water diffusion barrier from tumor cell membrane leading to the reduced ADC. Malignant tumors usually have the less ADC values due to active cell proliferation and high cell density. DW-MRI was first applied to the diagnosis of acute cerebral infarction, and then had important values in brain tumor, liver tumor, breast cancer and pancreatic tumor diagnosis and differential diagnosis [14]. Recently, the ADC was used to monitor the efficacy after chemotherapy of PDAC. Our studies showed ^{125}I seeds brachytherapy could induce the pathological changes of PDAC with significant necrosis [10]. The necrosis of tumor cells caused cell membrane rupture, cell density decrease, and residual tumor cells arranged loosely with increased cell gap. And then the pathological changes caused the ADC changes. In order to avoid potential interference introduced by central necrosis, the peripheral ADC values (within a 1-mm shell from the outer surface) were used for evaluation of response to therapy [15]. This study showed that after early ^{125}I seeds brachytherapy, the ADC values of tumor tissue were significantly increased. And the increase in ADC could be explained by the loss of overall cell density, decreased cell density, and increased extracellular space, which makes water molecules more free [6]. Okada et al. [16] also found pretreatment ADC value appeared to be a predictor of response to neoadjuvant therapy in patients with pancreatic carcinoma.

In the current study, we found a correlation between SUVmax and ADC values. SUVmax revealing tumor metabolism reflects cell proliferation and cell density. ADC values mainly reflect tissue cellularity and cell density. The negative correlation of SUV and ADC is thus reasonable since both parameters reflect cell density. The result is in agreement with several other studies. Sakane et al. [17] found ADC was significantly and negatively correlated with SUV in pancreatic adenocarcinomas. Other studies also indicated the correlation between SUV and ADC in lung cancer, cervical cancer, and rectal cancer [18–20]. They also got the similar results. These results indicate the comparability between SUVmax and ADC. But Goense et al. [21] found the tumor ADC and SUV showed negligible nonsignificant correlations in newly diagnosed esophageal cancer. Although the correlation between SUV and ADC may still be a controversial issue, these two parameters can accurately predict therapeutic response. Therefore, more work needs to be done in order to determine how to interpret these biomarkers in a complementary way.

We recognize several limitations to our study. Our in vivo study was obtained in a limited number of ro-

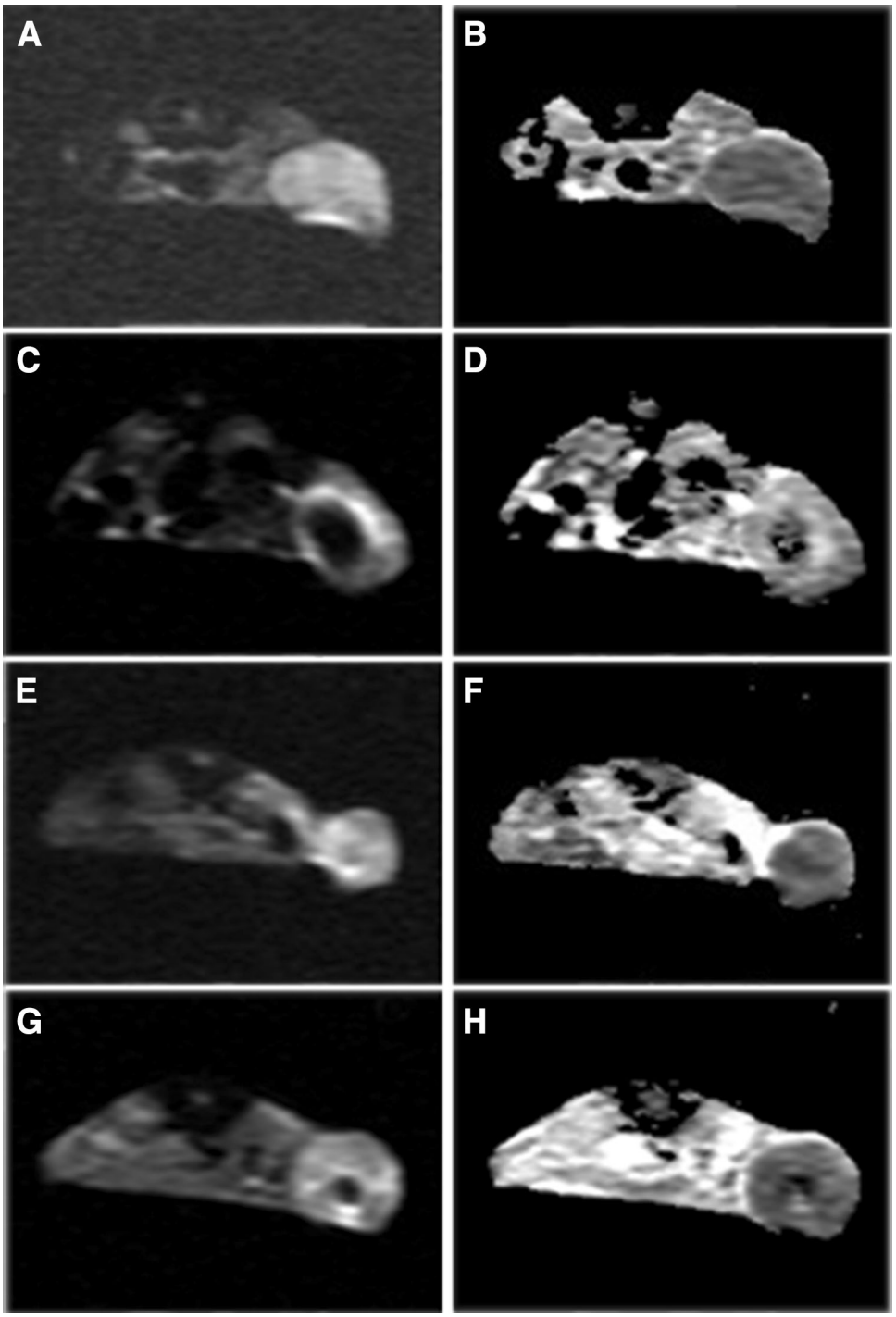

Fig. 2. The ADC change. **A** PDAC xenografts showed high signal intensity on DW-MRI. **B** And PDAC xenografts showed low signal intensity on ADC maps. **C** After the ^{125}I seeds brachytherapy, seeds showed no signal on DW-MRI. **D** And tumor showed slight hyperintensity on ADC maps in the ^{125}I seeds group after 5 days. **E** The DW-MRI of tumor in the control group at baseline. **F** The ADC maps of tumor in the control group at baseline. **G** The DW-MRI of tumor in the control group after 5 days. **H** The ADC maps of tumor in the control group after 5 days.

dents using PET/CT and DW-MRI. In addition, we used a clinical MR scanner with limited spatial resolution. Furthermore, we could not ensure the complete same location within tumor to measure the SUVmax and ADC. Future studies will have to perform the experiment by fusing MRI and PET/CT data sets or using PET/

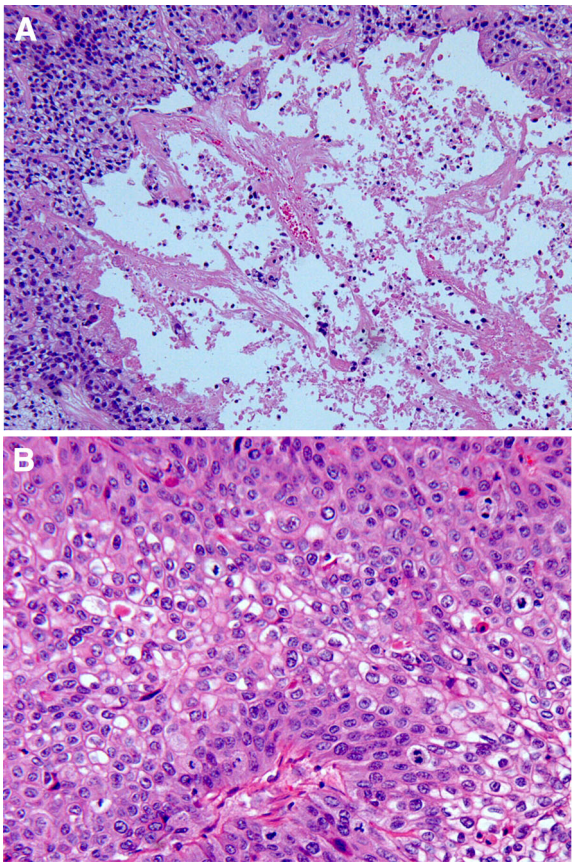

Fig. 3. H&E staining findings. **A** In the ^{125}I seeds group, there was significant necrosis around seeds with no cell structure and the residual tumor cells arranged loosely and appeared karyopyknosis. **B** In the blank seeds group, the tumor tissue showed no or a small amount of necrotic area, the tumor cells arranged closely, cells nuclear deeply dyed, and appeared more mitotic activity.

MRI. Moreover, future prospective studies using high-field animal MRI to enhance spatial resolution are needed.

In conclusion, early treatment monitoring of brachytherapy using the imaging modalities ^{18}F-FDG PET/CT and DW-MRI in a PDAC model is possible. This correlation between SUVmax and ADC indicates DW-MRI is potentially capable of offering similar information for treatment response evaluating as PET/CT does.

Acknowledgements This work was supported by Grants from the National Natural Science Foundation of China (81401455).

Compliance with ethical standards

Funding Yu Liu has received Grants from National Natural Science Foundation of China (81401455). For the remaining authors none were declared.

Conflict of interest All authors have no any financial and personal relationships with other people or organisations that could inappropriately influence (bias) their work.

References

1. Niu H, Zhang X, Wang B, et al. (1058) The clinical utility of image-guided iodine-125 seed in patients with unresectable pancreatic cancer. Br J Radiol 2016(89):20150573
2. Ergul N, Gundogan C, Tozlu M, et al. (2014) Role of (18)F-fluorodeoxyglucose positron emission tomography/computed tomography in diagnosis and management of pancreatic cancer; comparison with multidetector row computed tomography, magnetic resonance imaging and endoscopic ultrasonography. Rev Esp Med Nucl Imagen Mol 33(3):159–164
3. Min M, Lee MT, Lin P, et al. (1058) Assessment of serial multiparametric functional MRI (diffusion-weighted imaging and R2*) with (18)F-FDG-PET in patients with head and neck cancer treated with radiation therapy. Br J Radiol 2016(89):20150530
4. Tsuji K, Kishi S, Tsuchida T, et al. (2015) Evaluation of staging and early response to chemotherapy with whole-body diffusion-weighted MRI in malignant lymphoma patients: a comparison with FDG-PET/CT. J Magn Reson Imaging 41(6):1601–1607
5. Meier R, Braren R, Kosanke Y, et al. (2014) Multimodality multiparametric imaging of early tumor response to a novel antiangiogenic therapy based on anticalins. PLoS ONE 9(5):e94972
6. Zhang T, Zhang F, Meng Y, et al. (2013) Diffusion-weighted MRI monitoring of pancreatic cancer response to radiofrequency heat-enhanced intratumor chemotherapy. NMR Biomed 26(12):1762–1767
7. Tsuchida T, Morikawa M, Demura Y, et al. (2013) Imaging the early response to chemotherapy in advanced lung cancer with diffusion-weighted magnetic resonance imaging compared to fluorine-18 fluorodeoxyglucose positron emission tomography and computed tomography. J Magn Reson Imaging 38(1):80–88
8. Liu Y, Liu X, Gao W, et al. (2017) Combining DCE-MRI and 18F-FDG PET/CT for monitoring the efficacy of 125I seed brachytherapy in nude mice bearing pancreatic cancer xenografts. Chin J Med Phys 34(01):1–6 (Chinese)
9. Shah N, Zhai G, Knowles JA, et al. (2012) (18)F-FDG PET/CT imaging detects therapy efficacy of anti-EMMPRIN antibody and gemcitabine in orthotopic pancreatic tumor xenografts. Mol Imaging Biol 14(2):237–244
10. Liu Y, Wang Y, Tang W, et al. (2018) Multiparametric MR imaging detects therapy efficacy of radioactive seeds brachytherapy in pancreatic ductal adenocarcinoma xenografts. Radiol Med 123(7):481–488
11. Lim TY, Stafford RJ, Kudchadker RJ, et al. (2016) MRI characterization of cobalt dichloride-N-acetyl cysteine (C4) contrast agent marker for prostate brachytherapy. Tumour Biol 37(2):2219–2223
12. Hu S, Shi X, Chen Y, et al. (1058) Functional imaging of interstitial brachytherapy in pancreatic carcinoma xenografts using spectral CT: how does iodine concentration correlate with standardized uptake value of (18)FDG-PET-CT? Br J Radiol 2016(89):20150573
13. Arumugam T, Paolillo V, Young D, et al. (2014) Preliminary evaluation of 1'-[(18)F]fluoroethyl-β-D-lactose ([(18)F]FEL) for detection of pancreatic cancer in nude mouse orthotopic xenografts. Phys Med Biol 59(10):2505–2516
14. Schmid-Tannwald C, Schmid-Tannwald CM, Morelli JN, et al. (2013) Comparison of abdominal MRI with diffusion-weighted imaging to 68 Ga-DOTATATE PET/CT in detection of neuroendocrine tumors of the pancreas. Eur J Nucl Med Mol Imaging 40(6):897–907
15. Moestue SA, Huuse EM, Lindholm EM, et al. (2013) Low-molecular contrast agent dynamic contrast-enhanced (DCE)-MRI and diffusion-weighted (DW)-MRI in early assessment of bevacizumab treatment in breast cancer xenografts. J Magn Reson Imaging 38(5):1043–1053
16. Okada KI, Hirono S, Kawai M, et al. (2017) Value of apparent diffusion coefficient prior to neoadjuvant therapy is a predictor of histologic response in patients with borderline resectable pancreatic carcinoma. J Hepatobiliary Pancreat Sci 24(3):161–168
17. Sakane M, Tatsumi M, Kim T, et al. (2015) Correlation between apparent diffusion coefficients on diffusion-weighted MRI and standardized uptake value on FDG-PET/CT in pancreatic adenocarcinoma. Acta Radiol 56(9):1034–1041
18. Regier M, Derlin T, Schwarz D, et al. (2012) Diffusion weighted MRI and 18F-FDG PET/CT in non-small cell lung cancer

(NSCLC): does the apparent diffusion coefficient (ADC) correlate with tracer uptake (SUV)? Eur J Radiol 81(10):2913–2918
19. Brandmaier P, Purz S, Bremicker K, et al. (2015) Simultaneous [18F]FDG-PET/MRI: correlation of apparent diffusion coefficient (ADC) and standardized uptake value (SUV) in primary and recurrent cervical cancer. PLoS ONE 10(11):e0141684
20. Jeong JH, Cho IH, Chun KA, et al. (2016) Correlation between apparent diffusion coefficients and standardized uptake values in hybrid (18)F-FDG PET/MR: preliminary results in rectal cancer. Nucl Med Mol Imaging 50(2):150–156
21. Goense L, Heethuis SE, van Rossum PSN, et al. (2018) Correlation between functional imaging markers derived from diffusion-weighted MRI and 18F-FDG PET/CT in esophageal cancer. Nucl Med Commun 39(1):60–67